X-Ray Spectroscopic Studies on $Fe_{40}Ni_{38}Mo_4B_{18}$ Glassy Alloy During the Crystallization Process

G. Cocco and S. Enzo
Istituto di Chimica Fisica dell' Università di Venezia

L. Incoccia
Istituto di Struttura della Materia del CNR and PULS-Laboratori Nazionali di Frascati

and S. Mobilio
PULS-Laboratori Nazionali di Frascati

Z. Naturforsch. **38 a,** 1391 – 1395 (1983); received August 1, 1983

X-ray absorption spectroscopic measurements carried out on $Fe_{40}Ni_{38}Mo_4B_{18}$ glassy alloy undergoing crystallization are examined and discussed. Some trends in agreement with local-order rearrangements revealed by more conventional approaches (RDF and SAXS) have been found.

Peculiar features effected in the EXAFS and XANES spectra by increasing temperature treatments, have been interpreted on the ground of different strength of boron interaction with Ni and Fe atoms.

Introduction

In previous works, Radial Distribution Function analysis (RDF) [1] and Small Angle X-ray Scattering (SAXS) [2] have been concurrently employed to explore the short-range order and underlying texture of $Fe_{40}Ni_{38}Mo_4B_{18}$ glassy alloy during the crystallization process. Both techniques supported each other in the view that an amorphous phase demixes within the amorphous matrix at an early stage in the kinetic process. Moreover, it was determined that a more stable structural condition, namely the fcc γ-phase, is achieved by collective atomic rearrangement of five-fold-symmetry basic units, already present in the amorphous state.

In order to obtain further insight into the local order of this multicomponent system and in the absence of partial correlation functions, it is interesting to parallel the above studies by Extended X-ray Absorption Fine Structure (EXAFS) and X-ray Absorption Near Edge Structure (XANES) spectroscopies. These additional methods of investigation have become a promising local structure probe for non-crystalline materials [3–6], and, providing information on the local environment of a selected absorbing component in the amorphous structure, seems quite suitable for the problem in question. A preliminary EXAFS analysis on the FeNiMoB amorphous system, with varying Fe-Ni concentrations has been reported elsewhere [7]; here we present the results obtained on the same specimens previously studied by RDF and SAXS during crystallization with the primary concern of presenting the structural pattern emerging from the non-common combination of these very different X-ray techniques.

Reprint requests to G. Cocco, Istituto di Chimica Fisica dell' Università, Calle Larga S. Marta 2137. 30123 Venezia, Italy.

Experimental Details

Samples

Complete details of the specimen treatments are reported in (1) and (2). To summarize briefly, the samples (Metglas® 2826 MB) cut from ribbon rolls, were continuously heated under a protective argon atmosphere and quenched by direct admission of liquid nitrogen into a Differential Scanning Calorimetry (DSC) apparatus at 704.5, 711, 716 and 777 K, i.e. through the first DSC peak relevant to the (Ni, Fe, Mo) γ-phase appearance. Moreover, a further specimen was studied after annealing it at 963 K, i.e. beyond the second DSC peak pertinent to the complete crystallization of the system: at this stage, the residual amorphous part turns into a metastable boride, $(Fe,Ni,Mo)_{23}B_6$, having the complex cubic structure of the $Cr_{23}B_6$ compound [8].

0340-4811 / 83 / 1200-1391 $ 01.3 0/0. – Please order a reprint rather than making your own copy.

Measurements

EXAFS and XANES measurements were made, at room temperature, at the synchrotron facility (PULS) in the Frascati Laboratories. Synchrotron radiation emitted by the ADONE storage ring, working at 1.5 Gev, was monochromatized by a Si (111) channel-cut crystal. Typical electron current was 50 mA. EXAFS and XANES spectra for Ni and Fe K absorption edges were recorded in the same conditions for all the samples previously described. In the raw data reduction and data analysis [9], the same procedure was adopted for all the examined samples as regards background removal, transform ranges, effects of data cut-off and inverse transform range. EXAFS modulation is generally defined as [10]

$$\chi(k) = \frac{\mu - \mu_0}{\mu} = \sum_j \frac{N_j A_j(k)}{k r_j^2} \cdot e^{-2r_j/\lambda(k)} \sin[2k r_j + \varphi_j(k)], \quad (1)$$

where μ and μ_0 are the solid state and the atomic absorption coefficients, respectively; $k = [2m(E - E_0)/h^2]^{1/2}$ is the wave vector of the ejected photoelectron of energy E, E_0 being the absorption threshold; λ is the photoelectron mean free path; $A_j(k)$ is the backscattering amplitude for each of N_j neighbours of type j at a distance r_j away from the absorbing atom and φ_j is the total phase shift for the considered atom pair. The exponential term accounts for inelastic losses in the scattering process.

Results and Discussion

Representative radial correlation functions, obtained by transforming the $k\chi(k)$ reduced functions, are shown in Figs. 1 and 2 for the Fe-K and Ni-K edges, respectively, for the indicated annealing temperatures. Significant correlations rapidly fade after the first correlation sphere, and speculation beyond the nearest neighbours appears unreliable when dealing with complicated systems like these amorphous alloys [11]. Thus, with regard to the location of the main maximum, and restricting our initial attention to the sample as received, the atomic distributions in the environment of Fe and Ni atoms center at 2.04 ± 0.02 Å and 2.09 ± 0.02 Å, respectively, and appear in contrast with the value of 2.55 Å obtained by diffraction measurements [1]. The discrepancy between EXAFS and conventional RDF analysis was found in a great variety of metal-metalloid glasses [3, 8, 12–15] and was attributed to: i) a large contribution of the metal-metalloid pair correlation function to the first peak of the EXAFS Fourier Transform

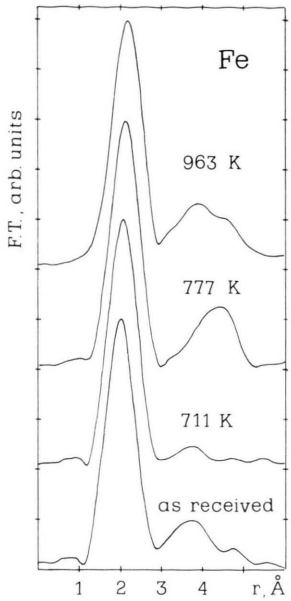

Fig. 1. Fourier Transforms of EXAFS on the iron K edge for the amorphous $Fe_{40}Ni_{38}Mo_4B_{18}$ undergoing crystallization. FT's of the $k\chi(k)$ reduced functions were computed over the finite k range 3 to 12 $Å^{-1}$.

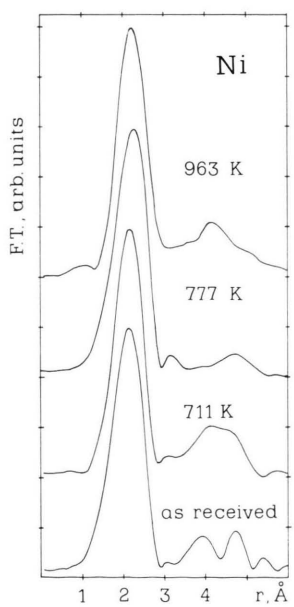

Fig. 2. Ni-K edge FT's of EXAFS signals for the specimens of Figure 1.

(FT), [16], or ii) an asymmetric metal-metal pair distribution function [17]. The discrimination between the above models is a hard task in these multicomponent alloys, and we will not discuss it here. Rather, it may be pertinent to note the difference in the bond distance obtained at the Fe and Ni edges: this feature appears consistent with the previous results [7] and, accordingly, different average coordination around the two absorbing atoms may be advanced. Furthermore we want to focus attention on the changes in the EXAFS spectra as the system evolves towards crystallization, monitoring the first peak position in the FT (Table 1). The position of the dominant maximum in the Ni-K spectra remains approximately constant for samples annealed up to 716 K, while the samples annealed at 777 K display an increase of 0.08 Å with respect to lower-temperature treated samples. The Fe spectra, on the other hand, show a progressive increase in the peak position up to 777 K; moreover a further shift up to 2.22 Å occurs for the sample annealed beyond the second DSC exotherm only for the Fe spectrum. All data being subjected to the same collection and reduction procedures, these peak shifts seem significant.

In order to understand these EXAFS data we recall briefly some RDF and SAXS results. The RDF analysis showed that the sample treated at 704.5 K maintains the general features of the sample as received and that only relaxation processes are accomplished at this stage of heat treatment. Although no important short range order rearrangements are therefore involved, the SAXS integrated intensity, varying with heat treatment, concurrently suggests that the system is engaged in the early stage of phase demixing. Further, even though the constancy of the integrated intensity is already reached for the sample treated at 711 K, thus manifesting accomplishment of the nucleation process, the related separated phases still retain an amorphous configuration, as shown by lack of crystalline details in the pertinent structure factor and by RDF features. At this thermal stage, in fact, progress toward a more definite structural state takes place through topological arrangements, without metric changes between the neighbouring atoms. Fitting this structural frame reasonably well, the relevant EXAFS features do not change within this field of thermal treatment, supporting a constant distance of atomic distribution in the nearest-neighbour coordination sphere. It may be noted that these results are in keeping with EXAFS findings of Wong et al. [18] for Fe-Ni based amorphous alloys. Particularly, it has been reported that annealing up to 598 K does not modify the local environment of Fe and Ni in $Fe_{40}Ni_{40}B_{20}$ as far as metrical values are concerned.

Table 1.

Sample	First maximum location in the Fourier Transform (Å)	
	Fe K edge ($E_0 = 7112$ eV)	Ni K edge ($E_0 = 8333$ eV)
As received	2.04	2.09
704 K	2.04	2.08
711 K	2.08	2.08
716 K	2.08	2.10
777 K	2.14	2.16
963 K	2.22	2.16

Returning to $Fe_{40}Ni_{38}Mo_4B_{18}$, a particle-coarsening mechanism occurs in samples annealed at higher temperatures: according to the evolution of the particle size distribution functions from SAXS, a critical size is achieved for which five-fold symmetry is no longer allowed. Concurrently, fcc domains appear in the samples treated up to 716 and 777 K, where the crystalline arrangement is now clearly recognizable. It is here that the fcc-γ-solid solution segregates, without boron, from the still amorphous matrix. At this stage the environment of the Ni atoms, present for the most part in the solid solution, appears to have reached its final configuration, while Fe atoms are still in a two-phase site: the crystalline solid solution and the amorphous matrix with boron. When the residual amorphous part turns into the second crystalline phase, i.e. the metastable $(FeNiMo)_{23}B_6$ for which a complex cubic form has been resolved, the final shift at 2.22 Å is observed in the Fe FT. On the basis of only qualitative considerations, the application of the Fe-Fe phase shift correction to the position of the maximum of the FT yields the value of ~ 2.55 Å very close to the diffraction results, manifesting the crystalline environment of Fe atoms.

For convenience of further consideration, XANES measurements were also performed. Figures 3 and 4 show the near edge structures of Fe and Ni as well as the relevant first derivatives. As can be seen, the

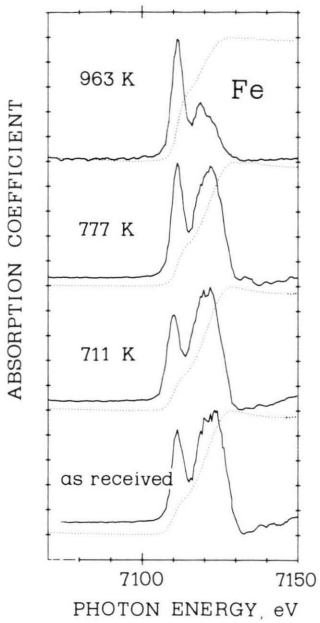

Fig. 3. Experimental trend of absorption coefficients (dotted line) and their first derivative (full line) for Fe XANES spectra of specimen studied.

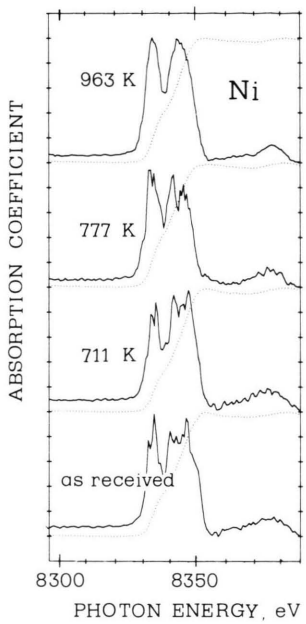

Fig. 4. Experimental trends of absorption coefficients (dotted line) and their first derivative (full line) for Ni XANES spectra of specimen studied.

Fe K XANES spectra display a behaviour which changes with thermal treatment. The ratio of the first to second peak increases with increasing temperature, and only in the case of the sample annealed after the second DSC peak does the spectrum approach that of crystalline Fe. The reduction of the first structure in the edge shape with respect to crystalline Fe has recently been observed for the $Fe_{40}Ni_{38}B_6P_{14}$ amorphous system, where a strong reduction of intensity of the first peak in the XANES spectra was observed, due to the metalloid presence [19]. This peculiar feature has been related to a charge transfer from B to Fe atoms, inducing a decrease of the empty density of state of the metal. Thus the changes in the XANES of Fe shows that the initial Fe-B privileged interaction becomes less important during the γ-phase appearance owing to the gradual impoverishment of iron in the amorphous matrix.

As far as the Ni K edges are concerned, the first derivative of the experimental absorption coefficients does not seem to display important changes with thermal treatment. This result confirms that the average environment of Ni atoms does not change appreciably upon crystallization. The avoidance of Ni by boron atoms is supported by the edge features, which do not show the decrease of strength of the first transition with respect to crystalline Ni. When the Ni atoms are coordinated by metalloid atoms (as in the amorphous NiP, for example) an effect similar to the one at the Fe edge is present [20].

The results of the present work could be interpreted on the ground of the different strength of boron interaction with Ni and Fe respectively. The formation heats of M_2B, MB and MB_2 borides of Ni are predicted to be at least 15% lower than those of Fe [21]. Moreover, nickel segregates preferentially during the first stage of crystallization in the boron-free fcc solid solution [22] leaving out boron in the still amorphous matrix. Further observations can be made about the stabilizing effect of Mo on the complex $Cr_{23}B_6$-type boride in the presence of a concentration of at least 15% at. Ni [23]. Depending on the Mo content, a minimum crystallization temperature and a maximum crystallization heat were found for a content of 4–5% at. Mo in the concentration range within which the $Cr_{23}B_6$-type boride formation is allowed. Moreover, especially important, some Ni-Mo ordering in the alloys has been surmised and the hypothesis that Ni-Mo pairs could already be present in the amorphous

state has been conclusively advanced to account for the whole thermodynamic and kinetic data set [23] and for the relevant X-ray absorption results pertinent to the $Fe_{78-x}Ni_xMo_4B_{18}$ ($x = 38, 20, 10, 0$) system [7]. Finally, it is to be remarked that the formation of intermetallic compounds such as $MoNi_4$ and $MoNi_3$ in the equilibrium phase diagram is indicative of the strong tendency toward NiMo coupling.

Some new details emerge consistent with and supporting previous accounts and it appears to us that the crystallization behaviour of the $Fe_{40}Ni_{38}Mo_4B_{18}$ glassy alloy has been clarified. When XANES and EXAFS results are paralleled by complementary techniques and the occurring phenomena are regarded from different points of view, it is possible to acquire a satisfactory understanding of the structural conditions and fine chemistry involved in spite of the complex nature of the system under study.

Acknowledgements

The authors are indebted (particularly G. C.) to Professors A. Lucci and L. Battezzati for fruitful discussions and permanent support in the course of this work. – Thanks are due to L. Moretto for technical assistence. – This work has been supported by C. N. R. (Progetto Finalizzato Metallurgia).

[1] G. Cocco, L. Schiffini, A. Lucci, and C. Antonione, J. Non-Cryst. Solids **50,** 359 (1982).
[2] G. Cocco, L. Schiffini, L. Battezzati, and A. Lucci, J. Non-Cryst. Solids **54,** 301 (1983).
[3] J. Wong, Metallic Glasses I, H. S. Güntherodt and H. Beck Eds., Springer-Verlag, Berlin 1981, p. 225 and references therein.
[4] T. M. Hayes and I. B. Boyce, Extended X-ray absorption fine structure spectroscopy, Solid State Physics **37,** p. 137, H. Erenreich, F. Seitz, and D. Turnbull Eds., Academic Press, New York 1982.
[5] D. Raoux, A. M. Flank, and A. Sadoc, Exafs and Near Edge Structure, A. Bianconi, L. Incoccia, and S. Stipcich Eds., Springer-Verlag, Berlin 1982, p. 232.
[6] P. H. Gaskell, D. M. Glover, P. J. Durham, and G. N. Greaves, J. Phys. C.: Solid State Phys. **15,** L597 (1982).
[7] F. Comin, L. Incoccia, S. Mobilio, and N. Motta, Exafs and Near Edge Structure, A. Bianconi, L. Incoccia, and S. Stipcich Eds., Springer-Verlag, Berlin 1982, p. 292.
[8] U. Herold and U. Foster, Z. Metal. **69,** 325 (1978).
[9] S. Mobilio, F. Comin, and L. Incoccia, Internal Report LNF-82/19 (NT).
[10] P. A. Lee, P. H. Citrin, P. Eisenberger, and B. M. Kincaid, Rev. Mod. Phys. **53,** 769 (1981).
[11] P. Eisenberger and G. S. Brown, Solid State Commun. **29,** 481 (1978).
[12] L. Logan, Phys. Stat. Sol. (a) **32,** 361 (1975).
[13] G. S. Cargill III, Proc. 4th Int. conf. on Rapidly Quenched Metals, Vol. I, T. Masumoto and K. Suzuki Eds., The Japan Institute of Metals, Doba Arakami, Sendai, Japan 1982, p. 389.
[14] A. M. Flank, P. Lagarde, D. Raoux, J. Rivory, and A. Sadoc, ibidem, p. 393.
[15] H. Maeda, H. Terauchi, N. Kamijo, M. Hida, and K. Osamura, ibidem, p. 397.
[16] G. S. Cargill III, W. Weber, and R. F. Boehme, Exafs and Near Edge Structure, A. Bianconi, L. Incoccia, and S. Stipcich Eds., Springer-Verlag, Berlin 1982, p. 277.
[17] M. De Crescenzi, A. Balzarotti, F. Comin, L. Incoccia, S. Mobilio, and N. Motta, Solid State Commun. **37,** 921 (1981).
[18] J. Wong, F. W. Lytle, R. B. Gregor, H. H. Liebermann, J. L. Walter, and F. E. Luborsky, Proc. 3rd Int. Conf. of Rapidly Quenched Metals, Vol. II, Sussex University, 1978, p. 345.
[19] M. De Crescenzi, A. Balzarotti, F. Comin, L. Incoccia, S. Mobilio, and D. Bacci, J. Phys. **41,** C8-238 (1980).
[20] P. Lagarde, J. Rivory, and G. Vlaic, J. Non-Cryst. Solids, to appear.
[21] A. K. Niessen and F. R. De Roer, J. Less Common Metals **82,** 75 (1981).
[22] A. Lucci, L. Battezzati, C. Antonione, and G. Riontino, J. Non-Cryst. Solids **44,** 287 (1981).
[23] L. Battezzati, C. Antonione, and A. Cossolo, Z. Metallkde. **73,** 185 (1982).